Chemistry Europe
European Chemical Societies Publishing

WILEY VCH

Excellence in Chemistry Research

Announcing our new flagship journal

- Gold Open Access
- Publishing charges waived
- Preprints welcome
- Edited by active scientists

Meet the Editors of *ChemistryEurope*

Luisa De Cola
Università degli Studi di Milano Statale, Italy

Ive Hermans
University of Wisconsin-Madison, USA

Ken Tanaka
Tokyo Institute of Technology, Japan

ChemPlusChem

Research Article
doi.org/10.1002/cplu.202300109

Chemistry Europe
European Chemical Societies Publishing

www.chempluschem.org

Cu-MOF-808 as a Sensing Material for Gaseous Hydrogen Sulfide

Nele Marquardt,[a] Melina Dahlke,[a] and Andreas Schaate*[a, b]

The selective detection of hydrogen sulfide (H_2S) is an important task because of its potentially hazardous effects not only on the environment but also on human health. Here, we present the zirconium-based MOF-808, which was modified with copper salts, as a colorimetric sensor material for the visible, reversible and sensitive H_2S detection at room temperature. The copper cations, which are incorporated in the oxidation state +II, are installed at the inorganic building units (IBUs) of the framework so that they are accessible for interactions with H_2S. The activated copper doped MOF-808 powder shows significant and fast color change in the presence of H_2S, which can be detected by UV-vis spectroscopy. Moreover, the detection process is reversible by heating the material to 120 °C under ambient conditions leading to its decolorization. The detection performance of the material was studied by in situ UV-vis measurements in a reaction chamber. The material was able to respond to 100 ppm H_2S in several cycles of exposure and heating to 120 °C under moist air conditions in a defined wavelength range. This reversibility is very uncommon for copper-based H_2S sensing reactions and highlights the potential of MOFs as selective sensing materials.

Introduction

Hydrogen sulfide is a colorless and toxic gas with potentially harmful impacts on the environment and human health. For example, a surpassing of the normal H_2S level in cells (10 μM to 100 μM) can cause different diseases like Alzheimer or cancer. Moreover, concentrations in the range of 5 ppm in the surrounding area can lead to irritations of the eyes, nose and throat and at ~30 ppm, the smell of the gas is no longer perceptible.[1] Hence, the detection of H_2S is urgently needed and often realized by sensor systems based on resistor changes of a material which reacts with H_2S. Semiconductor metal-oxides are the most popular sensor systems even though they need high working temperatures (100 to 400 °C) and they often lack selectivity.[2]

In order to obtain more selective sensor materials, metal-organic frameworks (MOFs) represent a promising material class for selective reactions with H_2S at room temperature.[3] The benefit in this context is their modular construction which enables the tailored adjustment to the desired applications. Until now, many reports about MOFs as sensing materials for H_2S exist, especially detection systems based on a fluorescence turn-on. This fluorescence change is caused for example by the reduction of functional groups ($-N_3$ or $-NO_2$) at the linker molecules by H_2S to amino groups.[1b,4]

However, most of these MOF materials are not able to detect gaseous H_2S. The detection processes were often performed in buffered ethanolic or aqueous solution and instead of gaseous H_2S, sulfide-containing salts like Na_2S were used for the evaluation of the sensor material.[5] In solution, Na_2S dissociates into the deprotonated species HS^- which is required for the reaction.[6]

Other detection methods, which are also based on fluorescence turn-on, take advantage of the reactivity of H_2S with metal cations. For instance, copper cations can form complexes with the linker molecules of porphyrin-based MOFs which quenches their fluorescence. The exposure to H_2S leads to the recovery of the fluorescence because of the formation of CuS and the resulting removal of the copper cations from the linker.[3] Moreover, the presence of copper cations can lead to the quenching of the fluorescence of rare-earth metal cations which are installed in the same framework. In this context, Eu^{3+} and Cu^{2+} can be inserted post-synthetically on free carboxylic acid functions of the linker molecules of MIL-100(In) films. The coordinated Cu^{2+} cations hinder the antenna effect between the organic ligand and lanthanide cations. When CuS is formed through the reaction with H_2S, the fluorescence is turned on again because the removal of the copper cations from the linker molecules restores the energy transfer to the Eu^{3+} cations.[7] This principle of CuS formation was also utilized in a colorimetric-based *mixed-linker* MOF sensor for gaseous H_2S including coordinated Cu^{2+} cations at the azo-groups of the linker molecules. Here, a significant color change of the material from green to black can be observed in presence of H_2S.[8] All

[a] N. Marquardt, M. Dahlke, Dr. A. Schaate
Leibniz University Hannover
Institute of Inorganic Chemistry
Callinstr. 9
30167 Hannover (Germany)
E-mail: andreas.schaate@acb.uni-hannover.de
[b] Dr. A. Schaate
Cluster of Excellence PhoenixD (Photonics, Optics and Engineering – Innovation Across Disciplines)
Leibniz University Hannover
30167 Hannover (Germany)

Supporting information for this article is available on the WWW under https://doi.org/10.1002/cplu.202300109

mentioned MOF sensor systems have the disadvantage that they are not reusable because the detection procedure is based on irreversible reactions of the material with H_2S.

Reversible detection cycles were reported with rare-earth metal based *fum*-**fcu**-MOF thin films on capacitive interdigitated electrodes showing changes in permittivity upon gas adsorption. The highest change in capacity was observed in the presence of H_2S. To evaluate the cross-sensitivity of this material with other compounds, only one other reactive gas, NO_2, was examined.[9]

We want to design a sensor material for the visible, reversible, and sensitive H_2S detection at room temperature taking advantage of a selective reaction with H_2S. Additionally, the regeneration of the material should be easy to perform.

The reaction of Cu(II) cations and H_2S was already investigated by Elias et al.[10] in the context of removing H_2S from wine. They examined the mechanisms by adding Cu(II) cations to a model wine solution containing H_2S and other thiol compounds. They observed the formation of Cu–S-complexes resulting in the oxidation of H_2S and reduction of Cu(II) to Cu(I). The reaction of Cu(I) with oxygen leads to the reoxidation of the metal cations. So, H_2S is able to initially oxidize and no insoluble copper sulfide was formed during this process. The transfer of this kind of redox reaction between copper cations and H_2S on MOF materials possibly enable a reversible, colorimetric based detection process.

For this purpose, we report here our results for copper functionalized MOF-808, in view of its potential to serve as a sensor material for gaseous H_2S with a reversible detection process. Each Zr_6-cluster in MOF-808, $[Zr_6O_4(OH)_4]^{12+}$, is coordinated by six trimesic acid molecules (H_3btc), resulting in a **spn** topology. In consequence, six coordination sites at these inorganic building units (IBUs) are not coordinated by linker molecules but can be saturated for example by carboxylates of small acids like formic, acetic or benzoic acid. These so-called modulators[11] are commonly used to control the synthesis of the material and are located in the hexagonal pore windows after the synthesis.[12] They can be post-synthetically exchanged by other modulator molecules[13] or they can even be completely removed leading to the generation of so-called active sites.[13b,14] This means that the Zr_6-clusters are saturated with $-OH_2$ and $-OH$ groups instead of the monocarboxylates. These active sites can be functionalized with transition metal cations which are then coordinated by the oxygen atoms of the Zr-IBUs (see Figure 1). This functionalization was already reported with for example Cu^{2+}, Fe^{2+} and Fe^{3+} salts in *N,N*-Dimethylformamide (DMF) with the focus on applying the resulting materials in the field of catalysis.[15] Our strategy is to use this kind of functionalization with Cu cations in order to expose them in the framework in a way that makes a colorimetric and reversible detection of H_2S possible.

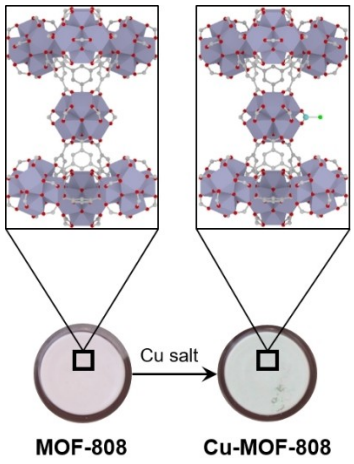

Figure 1. Schematic illustration of post-synthetic modification of MOF-808 structure with copper salts (top, color code: Zr: bluish-grey, O: red, C: grey, Cu: blue, Cl: green). Images of as-synthesized and copper modified MOF-808 powders (bottom).

Results and Discussion

Characterization of MOF-808 as starting material

MOF-808-X was synthesized as starting material with different modulators X, namely formic (FA), acetic (AA) and benzoic acid (BA) using modified protocols reported by Farha et al.[13b] or Lillerud et al.,[13a] respectively (see Experimental Section). In contrast to MOF-808-X (X = FA, AA), MOF-808-BA was synthesized by post-synthetical modification of MOF-808-AA by substituting the coordinating acetates by benzoates. The successful syntheses of the different materials were verified by PXRD (see Figure S1a in the Supporting Information) indicating high crystallinity of the obtained powders.

The amount of coordinating modulators was investigated by ^{1}H-NMR spectroscopy (Figure S2a in the Supporting Information) for each material. EDXS measurements were used to determine the amount of chloride anions saturating the Zr_6-clusters which is shown in the occupation diagram (see Figure S3 in the Supporting Information). Besides modulators and chlorides (both originating from the synthesis mixtures), water molecules and hydroxide anions are also able to coordinate and saturate the IBUs.[13a] The compositions of the directly synthesized MOF-808-X (FA, AA) are comparable with respect to the amount of the used modulator (~3.7) and the chloride anions coordinating to the IBUs. In contrast, the IBUs of the post-synthetically modified MOF-808-BA are nearly completely saturated by modulator molecules.

These coordinating modulators have an impact on the porosity and also on the hydrophilicity of the frameworks which was analyzed by argon (see Figure S4 in the Supporting Information) and water sorption measurements (Figure S5 in the Supporting Information). The isotherms show that all materials exhibit high surface areas depending on the coordinating modulator and are located in the same range as reported by Farha et al.[13b] The isotherms of MOF-808-X (X = FA,

AA) exhibit two steps. The second step is caused by the larger micropores with diameters of ~17.6 Å for MOF-808-FA and ~16.9 Å for MOF-808-AA. As expected, MOF-808-BA shows smaller pore diameters of ~9.5 to 10.9 Å because the benzoates located in the hexagonal pore windows reduce the pore diameters which is in correlation with the one step isotherm.[13a]

The hydrophilicity of the materials can be analyzed by water sorption measurements (see Figure S5 in the Supporting Information). MOF-808-FA shows the highest water uptake while MOF-808-BA exhibits the lowest (Figure S5a in the Supporting Information). The Henry diagram (Figure S5b in the Supporting Information) illustrates that the former framework is the most hydrophilic one. The tendency of the frameworks to adsorb water is in correlation with the polarity of the modulators saturating the IBUs (Figure S5c in the Supporting Information).[13b] All the shown frameworks are able to adsorb water without any loss of their crystallinity (Figure S1b in the Supporting Information).

Insertion of Cu cations into MOF-808-X

The insertion of copper cations was realized by post-synthetic modification (PSM) of MOF-808-X in DMF at 60 °C for 24 h using different copper salts, $CuCl_2 \cdot 2\ H_2O$ or $Cu(OAc)_2 \cdot H_2O$, respectively. In order to explore the impact of the modulators in the starting material on the functionalization process, all mentioned MOF samples were investigated using these two copper sources.

After this PSM, colored powders were obtained. The usage of $CuCl_2$ leads to lightly green samples while $Cu(OAc)_2$ leads to lightly blue powders which are shown in Figure S6 (in the Supporting Information). For the sake of brevity, samples which were functionalized with $CuCl_2 \cdot 2\ H_2O$ are referred to as Cu(Cl)-MOF-808-X and samples which were functionalized with < $Cu(OAc)_2 \cdot H_2O$ as Cu(OAc)-MOF-808-X.

The amount of incorporated copper cations was determined by EDXS and ICP measurements. The evaluated data from both methods show a high correspondence to each other.

The occupation diagrams which refer to the Zr_6-clusters (see Figure 2) display a loading of nearly one copper cation per cluster in Cu(OAc)-MOF-808-X. With $CuCl_2$ only half of the amount of copper cations is introduced to MOF-808-X.

Obviously, the choice of the copper salt has a higher influence on the amount of introducible copper cations than the attached modulators of the starting materials. Most likely, the pH value of the reaction mixture controls the PSM with copper cations.

While the chloride anions in the mixtures with $CuCl_2$ lead to a lower pH and a lower modification with copper cations, the higher pH value when using $Cu(OAc)_2$ has a beneficial effect on the insertion of copper cations. This thesis was confirmed by using mixtures of $CuCl_2$ and $Cu(OAc)_2$ with varying mole fractions between 0 and 1 for the modification with copper cations. Figure S7 (Supporting Information) illustrates the trend towards a lower copper cation loading by increasing the mole fraction of the more acidic $CuCl_2$.

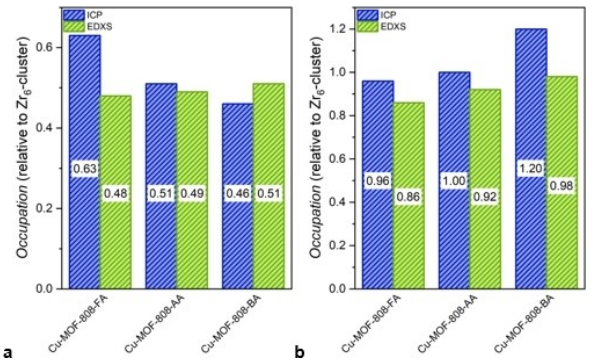

Figure 2. Amount of inserted copper cations relative to one Zr_6-cluster in Cu-MOF-808-X after the PSM of MOF-808-X (X = FA, AA, BA) using $CuCl_2 \cdot 2\ H_2O$ (a) or $Cu(OAc)_2 \cdot H_2O$ (b) as metal salts, respectively, calculated from ICP (blue) and EDXS (green) measurements.

The incorporation of copper cations into the framework was further analyzed with respect to the oxidation state of the cations inside the framework. The insertion of copper cations into MOF-808 using $Cu(OAc)_2$ was already performed by He et al.[3]

They reported that the copper cations are installed by coordinating to oxygen atoms from H_2O or OH^- anions saturating the IBUs. He et al.[15a] determined the oxidation state of the copper cations by XANES and concluded that they are present as Cu^{II} species.

We were able to determine the oxidation state of the introduced Cu cations by using electron spin resonance (EPR) spectroscopy. The advantage of this method in the study of Cu oxidation states is that Cu^{2+} cations can be explicitly distinguished from other oxidation species like Cu^+ cations in the spectrum. While Cu^+ is EPR 'silent', Cu^{2+} ions exhibit very characteristic EPR signals which can be found in the spectrum of all as-synthesized MOF powders, regardless of the starting materials. An exemplary spectrum of as-synthesized Cu(Cl)-MOF-808-FA is shown in Figure 3. The spectrum shows two signals $g_\perp$ (x,y) < $g_{||}$ (z) ($B_\perp > B_{||}$) which are characteristic for mononuclear Cu^{II} species with $S = 1/2$ exhibiting an axial

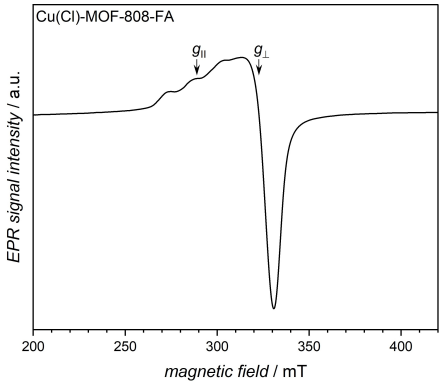

Figure 3. EPR spectrum of as-synthesized Cu(Cl)-MOF-808-FA showing two signals $g_\perp$ (x,y) < $g_{||}$ (z) ($B_\perp > B_{||}$) while $B_{||}$ signal is hyperfine split to four signals.

elongated coordination sphere in which one coordination axis is most often longer than the other two. The $B_{||}$ signal shows hyperfine splitting which could be caused by the interaction of the unpaired electron ($S = 1/2$) with the nucleus spin ($S = 3/2$) of Cu^{II}.[16]

In order to examine the influence of the PSM on the compositions of the resulting Cu-MOF-808-X materials, EDXS measurements were performed and digested samples were examined by ^{1}H NMR spectroscopy (Figure S2b and c). The results are illustrated in occupation diagrams (see Figure 4) with respect to the Zr_6-cluster.

The compositions changed drastically after PSM with the copper salts compared to the respective starting materials (Figure S3 in the Supporting Information) concerning the amount of modulators and chlorides. Additionally, there is also a significant amount of DMF present in the pores of the materials after PSM even though the samples were washed thoroughly with acetone after the modification procedure (Figure S2b and c in the Supporting Information).

In the case of the materials synthesized with $CuCl_2$, the amount of modulators were reduced after PSM (Figure 4a). The amount of modulator in Cu(Cl)-MOF-808-FA is reduced to ~2, in Cu(Cl)-MOF-808-AA to ~2.7 and in Cu(Cl)-MOF-808-BA to ~3.2 per IBU. The amount of chloride anions in the structure is in the same range for all samples considered. The chloride anions are able to saturate the sites at the IBUs, as already mentioned,[1,6] but we have to consider that they could also coordinate to the introduced copper cations.

If copper acetate were used as the metal salt, all samples include acetate after the procedure (see Figure 4b) which could be explained by the high excess of acetate during the PSM. In this case, the formate and benzoate modulators have been completely and partially removed, respectively, and replaced by acetates so that all Cu(OAc)-MOF-808-X samples contain a significant amount of acetate from 4.4 to 5.5. Regarding the amount of chloride anions, only a low amount remained at the IBUs originated from the starting MOF-808-X materials.

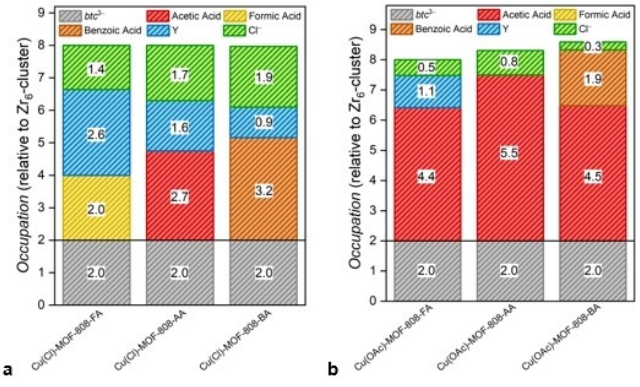

Figure 4. Composition of Cu(Cl)-MOF-808-X (X = FA, AA, BA) (a) and Cu(OAc)-MOF-808-X (b) relative to one Zr_6-cluster including the linker btc^{3-}, the modulators, chloride calculated from EDXS measurements and Y. Y represents the unidentified molecules saturating the rest of the free coordination sites of the Zr_6-clusters which could potentially be H_2O/OH^-.

The stability of the frameworks after the incorporation of copper cations was confirmed by PXRD (see Figure S8 in the Supporting Information). The peak positions of the samples after the procedure are unchanged with respect to those of the starting materials so that it can be stated that the introduced Cu cations have no influence on the overall structure of the framework. This is consistent with the assumption that they are coordinated to the IBUs and are thus placed in the pore windows.[15a]

The argon sorption measurements (Figure 5) confirm this, because the surface areas are reduced after PSM but the materials still remain porous which is an important requirement for the usage of the material for H_2S detection.

Regardless which metal salt was used during PSM, Cu-MOF-808-FA and -AA show quite similar surface areas which are reduced compared to the starting materials to ~1500 $m^2 g^{-1}$. The pore sizes are also in the same range, but slightly reduced after PSM, due to the introduction of copper cations. Cu(Cl)-MOF-808-BA and Cu(OAc)-MOF-808-BA exhibit a similar tendency in view to the surface areas which are reduced from ~1750 $m^2 g^{-1}$ to ~1300 $m^2 g^{-1}$ while the pore sizes are increased compared to the starting materials to ~12 Å and ~14 Å, respectively. A possible explanation for this increase in pore size is the reduction of the amount of benzoates pointing into the pores.

Exposure to H_2S

The preliminary testing of the responsivity of Cu doped MOF-808-X were performed by exposing the samples to gaseous hydrogen sulfide in covered beakers. The samples were placed in proximity to a screw-lid glass containing sulfuric acid to which sodium sulfide was added to start the evolution of H_2S. We observed a fast color change from green or blue, depending on the Cu-MOF-808-X used, to brown. These color changes were examined by ex situ UV-vis measurements (see Figure 6 and Figure S9 in the Supporting Information). After the H_2S exposure of the as-synthesized Cu-MOF-808-X samples, a general increase of the absorption takes place over a broad range from ~250 nm to ~650 nm which corresponds to the by-eye observed color change to brown. The exposure has no negative impact on the crystallinity of the materials which was verified by PXRD (see Figure S10 in the Supporting Information).

Before examining the reaction with H_2S in more detail, we want to show what other factors influence the UV-vis absorption of the MOF and how they can be optimized for the sensing process.

The rate of decolorization of the brown samples depends very much on the copper salt used, so we paid special attention to the influence of the counter anions that are introduced by the different precursors.

A main difference between the materials can be seen in the UV-vis spectra. In the case of materials synthesized with copper chloride, the spectra of the as-synthesized samples and the decolorized samples differ after exposure to H_2S. The maximum

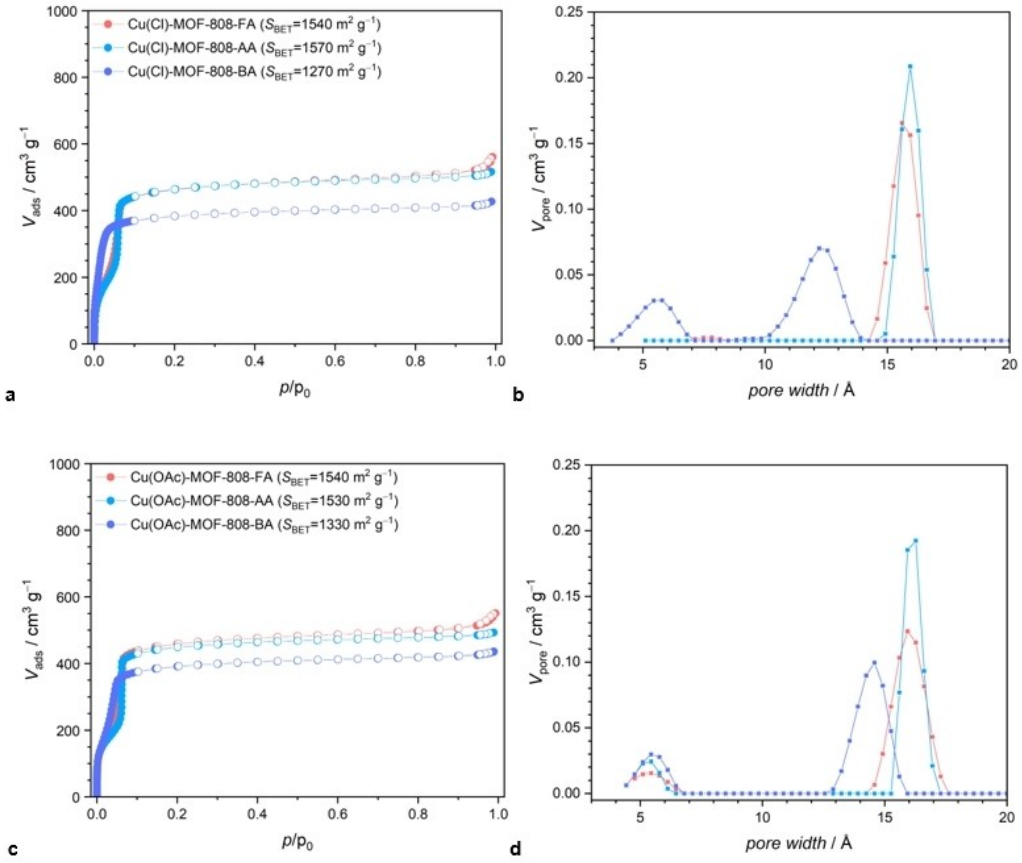

Figure 5. Argon adsorption isotherms at 87 K (a) and pore size distribution estimated by using non-localized density functional theory (NLDFT) (b) of Cu(Cl)-MOF-808-FA (red), -AA (blue) and -BA (violet) as well as of Cu(OAc)-MOF-808-FA (red), -AA (blue) and -BA (violet) (b,d).

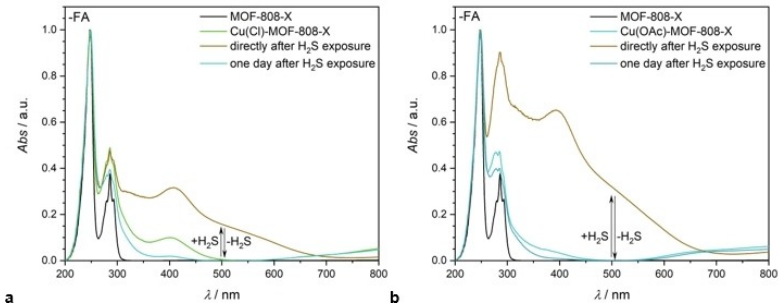

Figure 6. Normalized UV-vis spectra of MOF-808-FA and Cu(Cl)-MOF-808-FA (a) and Cu(OAc)-MOF-808-FA (b), respectively, before, directly and one day after H_2S exposure.

at ~400 nm, which is just present in spectra of as-synthesized samples, is especially observable for Cu(Cl)-MOF-808-FA (see Figure 6a, green curve). This maximum of absorption only occurs if the samples were synthesized with copper chloride, no sample that was synthesized with copper acetate showed this absorption (see Figure 6b and Figure S9c and d in the Supporting Information). So, the color of the material depends on the counter anion coordinated to the copper cations.

In order to confirm this, we stored Cu(OAc)-MOF-808-AA in a hydrogen chloride atmosphere. The UV-vis spectra before and after this procedure show a clear formation of a maximum at ~400 nm (see Figure S11 in the Supporting Information) which can be attributed to the presence of chlorides at the copper cations in the material. In order to quantify the amount of chlorides we used EDXS measurements (Figure S12 in the Supporting Information) which showed that the amount of chlorides is drastically increased from ~0.8 to ~2.6 per Zr_6-cluster after the HCl exposure.

The amount of chloride anions does not change, even after H_2S exposure, so they are permanent ligands during the sensing process. The results from ^{1}H NMR spectroscopy (Figure S12, Figure S13 in the Supporting Information) exhibit that the

amount of acetates did not change upon HCl exposure. Most likely the acetates are replaced by chlorides at the Cu cations but remain in the framework by saturating the IBUs.

We also investigated the impact of DMF concerning the color of the samples and the appearing features in the UV-vis spectra. For this purpose, we stored Cu(Cl)-MOF-808-FA in a DMF atmosphere. A color change to yellow could be observed. The UV-vis spectra before and after exposure (see Figure S14 in the Supporting Information) also show an increase of the absorption intensity in the range of ~400 nm. It has to be pointed out that this color change could only be observed for Cu(Cl)-MOF-808-X. In consequence, the color of the sample and therefore the features in the UV-vis spectrum are influenced by the coordination of DMF to the copper cations if chloride anions are also present as ligands. The maximum at ~400 nm in the as-synthesized Cu(Cl)-MOF-808-X can be eliminated by heating the sample to 120 °C in an oven under ambient conditions. The as-synthesized material transformed to a lightly blue powder after activation. This color change can be explained by the reduction of the amount of DMF by heating (see 2.4 in the Supporting Information) and the substitution of the ligand by water molecules under ambient conditions afterwards. This could be verified by the already shown impact of DMF on the UV-vis spectrum of the sample (Figure S14 in the Supporting Information) exhibiting the reverse color change. Another confirmation for the presence of water molecules after the activation procedure is given by the change of the shape of the EPR spectrum (see Figure 7, Figure S15 in the Supporting Information) compared to that of as-synthesized Cu(Cl)-MOF-808-FA (see Figure 3). After the activation of the material, an additional signal at ~316 mT appears in the EPR spectrum which is characteristic for a hydrated state.[17]

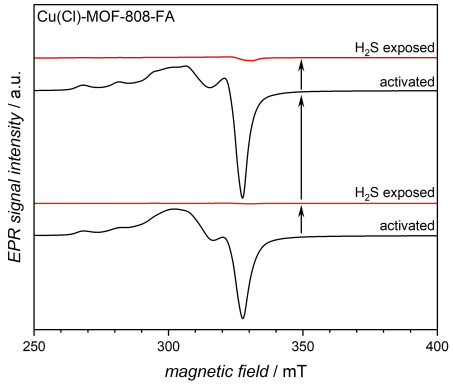

Figure 7. Reduction of Cu^{II} to Cu^{I} in Cu(Cl)-MOF-808-FA by exposure to H_2S and reoxidation by activation of the material at 120 °C illustrated by the significant change of the EPR signal intensity. The signal of the activated material.

In order to generate a fully reversible process for H_2S sensing, it is advantageous to use Cu(Cl)-MOF-808-X due to its better performance in terms of regenerability.

The colorization by H_2S exposure and decolorization which could be accelerated by the mentioned heating procedure can also be investigated by EPR spectroscopy and can be explained by the reduction of the Cu cations in the framework from Cu(II) to Cu(I). The reduction of copper based complexes[18] or enzymes[19] was already observed by other groups and measured for example by EPR spectroscopy.

The EPR spectrum of activated Cu(Cl)-MOF-808-FA clearly shows the signals of Cu^{2+} in the sample. Exposing the sample to H_2S leads to the loss of the characteristic signal of Cu^{2+} (see Figure 7) which can be assigned to the reduction of paramagnetic Cu^{2+} to EPR inactive Cu^{+} species. After activation, the EPR spectrum of the decolorized sample again shows the initial signals of Cu^{2+} indicating that the copper cations are oxidized again. This means that the so treated material can be used for the reversible, selective, cyclic detection of H_2S (see Figure 8).

In order to confirm that the presence of other gases does not lead to interfering signals during the H_2S detection, we exposed Cu(Cl)-MOF-808-AA also to other reactive gases like NH_3, NO_2, CO, CO_2 and SO_2. The material remains stable after these treatments (Figure S16a in the Supporting Information). These exposures in fact caused color changes of the sample but the significant shifts of the intensities in the UV-vis spectra (see Figure S16b in the Supporting Information) do not occur in the considered range for the H_2S detection.

The heat induced transformations of Cu-MOF-808-X and the cyclic H_2S exposures were further investigated by in situ UV-vis measurements.

In situ UV-vis measurements

Because of the fact that the detection process is reversible, we decided to perform in situ UV-vis measurements to investigate the responsivity behavior of the functionalized MOF towards H_2S in more detail.

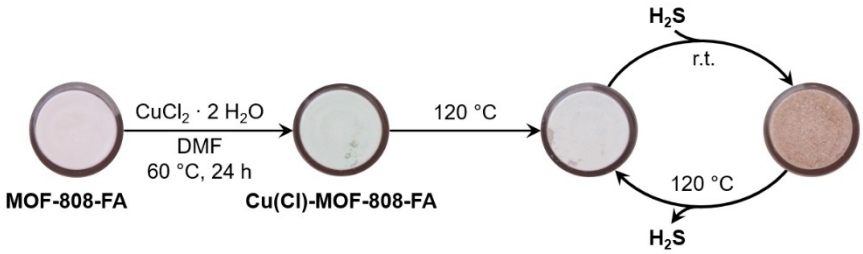

Figure 8. Functionalization procedure, activation and detection cycle of H_2S for Cu(Cl)-MOF-808-FA. Heating to 120 °C of as-synthesized Cu(Cl)-MOF-808-FA (lightly green colored material) leads to the activated lightly blue powder which can be used as a starting material for the detection cycle of H_2S. The exposure of H_2S results in a color change to brown which is reversible by heating to 120 °C.

The in situ UV-vis measurements were carried out by using a reaction chamber which can be streamed with H_2S, dry or moist air and was coupled to a heater and a cooling system to enable the adjustment of different working steps needed for the reversible detection process.

In the first step, the sample was heated to 120 °C under dry air conditions and afterwards cooled to room temperature under moist air conditions to get the activated MOF (see Figure S18a in the Supporting Information) as the starting material for the detection process. Details and observations during this activation procedure for Cu-MOF-808-FA can be found in the Supporting Information (see 2.4).

In a further step, we examined the activated Cu(Cl)-MOF-808-FA by in situ UV-vis measurements with the focus on its responsiveness to H_2S. For this purpose, the reaction chamber was streamed with gaseous H_2S (100 ppm) at room temperature and the average intensity change in the range of 505 to 510 nm was plotted against the time (Figure 9). The on-set is located at ~2.4 min after starting the gas flow through the chamber. After ~10 min, the intensity increases no longer and remains at a constant level. The decolorization was realized by in situ heating of the sample holder to 90 °C and subsequent cooling of the sample in a moist air gas flow. In contrast to Cu(OAc)-MOF-808-FA, the initial condition of the activated Cu(Cl)-MOF-808-FA could be fully regenerated (see Figure S20 in the Supporting Information) which shows that the H_2S sensing reaction is completely reversible using this material.

Cyclic H_2S exposures were performed to prove the reversibility of the sensing process and to investigate the responsiveness of the material which ranges in the area of 1.3 min to 2.2 min. The material shows reproducible results in view to the changes in mean intensities (see Figure S21 in the Supporting Information). The slight deviations are probably due to the fact that the instrument used for the in situ measurements is not specifically designed for sensing applications. Thus, the present results can only serve as an encouraging proof of concept for further investigations and the use of the material in a sensor system.[20]

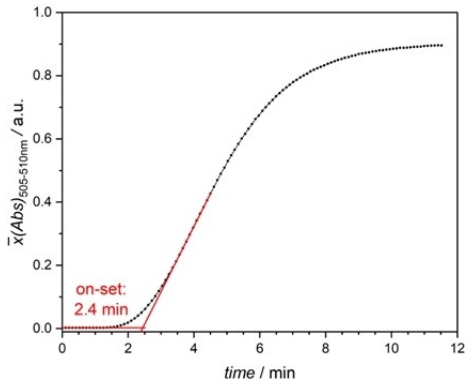

Figure 9. Responsiveness of the activated Cu(Cl)-MOF-808-FA to H_2S in time in consideration of the mean value of the measured absorption intensities in the range from 505 to 510 nm.

Conclusion

In conclusion, we present Cu(Cl)-MOF-808 as a fully regenerable sensing material for gaseous H_2S at room temperature. The presence of chloride anions as ligands coordinating to the introduced copper cations is essential for the reversibility of the process. The detection process is based on a reduction reaction in which Cu(II) cations installed at the IBUs of the framework are temporarily reduced to Cu(I) which was shown by EPR spectroscopy. The material can be fully regenerated which is accelerated when it is heated and subsequently cooled under moist air conditions. After this process, EPR spectroscopy shows that the copper cations are oxidized to Cu(II) again. Exposure to a stream of water vapor saturated air during the cooling process causes faster decolorization and regeneration of the material. The materials show comparable performances, also after several detection cycles, whereby the responsiveness ranges in a reproducible area from 1.3 to 2.2 min.

Overall, the incorporation of copper cations in MOF-808 and the fine tuning of the affinity of the material to H_2S by carefully choosing counter anions and modulators show the high adaptability of MOFs and underline the potential of this substance class for the application as selective sensor materials.

Experimental Section

Materials

Zirconium (IV) chloride (>99.5%, $ZrCl_4$, Sigma Aldrich), Benzene-1,3,5-tricarboxylic acid (95%, trimesic acid, H_3btc, $C_9H_6O_6$, Sigma Aldrich), *N*,*N*-dimethylformamide (≥99.8%, ACS reagent, DMF, C_3H_7NO, Sigma Aldrich), acetic acid (≥99.7%, ASC reagent, CH_3COOH, Sigma Aldrich), formic acid (~98%, HCOOH, Fluka Analytical), benzoic acid (≥99.5%, ASC reagent, C_6H_5COOH, Sigma Aldrich), hypochloric acid (37%, ACS reagent, HCl, Sigma Aldrich), acetone (technical, C_3H_6O, Fisher Chemical), copper (II) chloride dihydrate (>99%, $CuCl_2 \cdot 2\ H_2O$, Riedel-de-Haën), copper (II) acetate monohydrate (≥99.0%, $Cu(OAc)_2 \cdot H_2O$, Fluka), sulfuric acid (96%, H_2SO_4, ROTH), sodium sulfide nonahydrate (technical, $Na_2S \cdot 9\ H_2O$), ammonium carbonate (EMSURE, ACS reagent, $(NH_4)_2CO_3$, Sigma Aldrich), deuterium oxide (deuteration degree min. 99.95% for NMR spectroscopy, D_2O, Sigma Aldrich), Zr ICP standard solution ($ZrOCl_2$ 99.996%, 5% HCl, 0.5% HF, 1000 mg/L, ROTH), Cu ICP standard solution (Cu 99.999%, 2% HNO_3, 1000 mg/L, ROTH), nitric acid (ROTIPURAN Supra 69%, HNO_3, ROTH) were used as obtained. The gas exposure experiments were performed using a gas bottle from Linde GmbH including a mixture of H_2S (100 ppm) and N_2.

MOF syntheses

All water-based MOF-808-X syntheses were performed in round-bottom flasks under reflux conditions and stirring by a modified approach from Farha et al.[13b] (X = FA, AA) or Lillerud et al.[13a] (X = BA).

MOF-808-FA and MOF-808-AA

$ZrCl_4$ (3 mmol, 1 eq) and H_3btc (1 mmol, 0.33 eq) were dissolved in a mixture of conc. HCl (100 µL, 0.4 eq), formic (3.5 mL, 30.9 eq) or acetic acid (5 mL, 26.9 eq), respectively, and water (10 mL,

184.7 eq). The mixtures were heated in an oil bath to 110 °C for 24 h. The resulting white MOF-808-X powders were collected by centrifugation (6000 rpm, 10 min) and washed three times with water and two times with acetone. The powders were pre-dried at 60 °C for at least 2 h and further drying was performed at 120 °C.

MOF-808-BA

The synthesis of MOF-808-BA was realized by PSM of MOF-808-AA. Benzoic acid (9.83 mmol, 2.38 eq) was stirred in water (100 mL, 1342 eq) at 60 °C in an oil bath until almost complete dissolution. MOF-808-AA (0.691 mmol, 0.167 eq) was added to the solution and the mixture was further stirred at 60 °C for 24 h. The white powder was collected by centrifugation (6000 rpm, 10 min) and washed six times with water and one time with acetone. The product was pre-dried at 60 °C for at least 2 h and further drying was performed at 120 °C.

Post-synthetic modification of MOF-808-X with copper salts

The post-synthetic modification of MOF-808-X with copper salts was performed in DMF. $CuCl_2 \cdot 2\ H_2O$ or $Cu(OAc)_2 \cdot H_2O$ (1.61 eq), respectively, was dissolved in DMF (20 mL) by ultrasonication. MOF-808-X (300 mg, 0167 eq) was added to the green or blue solution, respectively, and heated to 60 °C in an oven for 24 h. The powder was obtained by centrifugation (6000 rpm, 10 min). The powders were washed with DMF until the supernatant remains colorless and then one time with acetone. The green or blue products, respectively, were dried at 60 °C.

Exposure to H_2S

For quick H_2S exposure experiments, 25 mg to 50 mg of the synthesized Cu-MOF-808-X powders filled in glass vessels were placed in a 250-mL beaker in combination with a glass vessel filled with conc. H_2SO_4. The gas evolution was realized by the addition of *ca.* 25 mg of Na_2S to the acid and the beaker was quickly covered by a Petri dish. During the first seconds of gas evolution, a significant color change from bluish or greenish, respectively, to different shades of brown happened. After one day at atmospheric conditions, the brown samples changed to bluish powders excluding the Cu(OAc)-MOF-808-BA sample. The Cu(Cl)-MOF-808-X samples generally showed a faster decolorization after H_2S exposure. The removal of H_2S could be accelerated by heating the exposed samples to 120 °C in an oven.

Inductively coupled plasma optical emission spectrometry

ICP-OES measurements were performed by the ICP Expert II software at a Varian Vista Pro ICP-OES from Labexchange. The calibration curve was drawn up with 1000 mg/L Zr and Cu standard solutions in a range from 10 to 50 mg/L and 1 to 20 mg/L, respectively. First, 3 mg of the samples were dissolved in 0.5 mL 1 M $(NH_4)_2CO_3$ solution under stirring overnight and then acidified with 2 mL 69% HNO_3. The solution was diluted to 25 mL in a volumetric flask by 3% HNO_3.

Electron paramagnetic resonance spectroscopy

EPR spectroscopy were performed using a Magnettech MS 5000 from Bruker. The spectra were measured using the software MiniScope MS5000 by Freiberg Instruments by filling the powder samples in a capillary tube with a diameter of 4 mm. The measurement was performed in the range from 240 mT to 420 mT with a frequency of 100 Hz with a microwave power of 50 Hz.

^{1}H NMR Spectroscopy

^{1}H NMR spectroscopy was conducted at room temperature at 400 MHz by using a Bruker BioSpin. The samples were dissolved in 0.6 mL 1 M $(NH_4)_2CO_3$ solution in D_2O under stirring overnight. The analysis of the spectra was realized by TopSpin 4.0.9 software.

Powder X-ray diffraction

PXRD was carried out by using a Stoe Stadi P transmission diffractometer operating with Ge(111)-monochromatized $CuK_{\alpha1}$ radiation ($\lambda = 1.54056$ Å) and position sensitive Mythen 1 K Detector.

Physisorption measurements

Argon physisorption isotherms were measured at 87 K by a Micromeritics 3Flex instrument. The samples were solvent-exchanged by soaking in acetone for *ca.* 24 h and outgassed at 50 °C for Cu-MOF-808-X or 120 °C for MOF-808-X, respectively, in vacuum immediately prior the measurement. The determination of the BET surface area was realized by the 3Flex Version 5.02 software enabling the assessment of the relative pressure range for BET according to the Rouquerol theory. The pore width distribution was also investigated by NLDFT for cylindrical pore geometry.

Water physisorption isotherms were recorded at 298 K by a 3P instrument. The samples were outgassed at 120 °C in vacuum immediately prior the measurement. The Henry constant K_H and α were determined based on the isotherms and were transformed into the Henry plot.

Scanning electron microscopy and energy-dispersive X-ray spectroscopy

SEM measurements were performed on a Jeol JSM-6610LV scanning electron microscope using secondary electrons at 20 kV. The measurements were performed with spot size adjusted to 36 and the working distance was 10 mm.

EDX spectra were measured with an integrated EDX-detector XFlash Detector 410-M with spot size over 50 and measurement tie of 10 min. The data were quantitatively evaluated in the Esprit software.

Few of the powder was put on a holder with carbon tape and the samples were gold-sputtered in Ar plasma for 30 s and 30 mA at Cressington Sputter Coater 108 auto.

UV-vis spectroscopy

The samples were measured before and after H_2S exposure and removal as powders via UV-vis spectroscopy in the range from 200 to 800 nm. The measurements were performed on a Cary4000 from Agilent Technologies by using a Praying Mantis Diffuse Reflection Accessory from Harrick.

In situ UV-vis spectroscopy measurements with reaction chamber and heater

The in situ UV-vis spectroscopy measurements were performed on a Cary4000 from Agilent Technologies in a reaction chamber which was placed in the Praying Mantis Diffuse Reflection Accessory from Harrick. The gas stream through the chamber was controlled by using a flow regulator which could be switched between air and H_2S (100 ppm in N_2) from gas cylinders. The flow could also be switched to moist air. The reaction chamber was also connected to a temperature controller (Watlow 998, Harrick) and a water-cooling unit enabling in situ heating and cooling of the sample in the chamber. Cycled measurements were performed in the range of 200 nm to 600 nm or 505 to 510 nm, respectively.

Acknowledgements

General support and fruitful discussions with Prof. Dr. Peter Behrens are gratefully acknowledged. The authors would like to thank the Hannover School for Nanotechnology (hsn) which is based in the Laboratory for Nano and Quantum Engineering (LNQE) for financial funding. Open Access funding enabled and organized by Projekt DEAL.

Conflict of Interest

The authors declare no conflict of interest.

Data Availability Statement

The data that support the findings of this study are available in the supplementary material of this article.

Keywords: colorimetric sensors · copper · gas sensors · hydrogen sulfide · metal-organic frameworks

[1] a) M. S. Shah, M. Tsapatsis, J. I. Siepmann, *Chem. Rev.* **2017**, *117*, 9755–9803; b) S. S. Nagarkar, T. Saha, A. V. Desai, P. Talukdar, S. K. Ghosh, *Sci. Rep.* **2014**, *4*, 7053.
[2] N. Joshi, T. Hayasaka, Y. Liu, H. Liu, O. N. Oliveira, L. Lin, *Mikrochim. Acta.* **2018**, *185*, 213.
[3] Y. Ma, H. Su, X. Kuang, X. Li, T. Zhang, B. Tang, *Anal. Chem.* **2014**, *86*, 11459–11463.
[4] a) X. Zhang, J. Zhang, Q. Hu, Y. Cui, Y. Yang, G. Qian, *Appl. Surf. Sci.* **2015**, *355*, 814–819; b) S. S. Nagarkar, A. V. Desai, S. K. Ghosh, *Chem. Eur. J.* **2015**, *21*, 9994–9997.
[5] a) R. Dalapati, S. N. Balaji, V. Trivedi, L. Khamari, S. Biswas, *Sens. Actuators B* **2017**, *245*, 1039–1049; b) A. Legrand, A. Pastushenko, V. Lysenko, A. Geloen, E. A. Quadrelli, J. Canivet, D. Farrusseng, *ChemNanoMat* **2016**, *2*, 866–872; c) S. Nandi, H. Reinsch, S. Banesh, N. Stock, V. Trivedi, S. Biswas, *Dalton Trans.* **2017**, *46*, 12856–12864.
[6] H. A. Henthorn, M. D. Pluth, *J. Am. Chem. Soc.* **2015**, *137*, 15330–15336.
[7] J. Zhang, F. Liu, J. Gan, Y. Cui, B. Li, Y. Yang, G. Qian, *Sci. China Mater.* **2019**, *62*, 1445–1453.
[8] M. Schulz, N. Marquardt, M. Schäfer, T. Heinemeyer, A. Schaate, *RSC Adv.* **2020**, *10*, 12334–12338.
[9] O. Yassine, O. Shekhah, A. H. Assen, Y. Belmabkhout, K. N. Salama, M. Eddaoudi, *Angew. Chem.* **2016**, *128*, 16111–16115; *Angew. Chem. Int. Ed.* **2016**, *55*, 15879–15883.
[10] a) G. Y. Kreitman, J. C. Danilewicz, D. W. Jeffery, R. J. Elias, *J. Agric. Food Chem.* **2017**, *65*, 2564–2571; b) G. Y. Kreitman, J. C. Danilewicz, D. W. Jeffery, R. J. Elias, *J. Agric. Food Chem.* **2016**, *64*, 4095–4104.
[11] A. Schaate, P. Roy, A. Godt, J. Lippke, F. Waltz, M. Wiebcke, P. Behrens, *Chem. Eur. J.* **2011**, *17*, 6643–6651.
[12] H. Furukawa, F. Gándara, Y.-B. Zhang, J. Jiang, W. L. Queen, M. R. Hudson, O. M. Yaghi, *J. Am. Chem. Soc.* **2014**, *136*, 4369–4381.
[13] a) E. Aunan, C. W. Affolter, U. Olsbye, K. P. Lillerud, *Chem. Mater.* **2021**, *33*, 1471–1476; b) X. Liu, K. O. Kirlikovali, Z. Chen, K. Ma, K. B. Idrees, R. Cao, X. Zhang, T. Islamoglu, Y. Liu, O. K. Farha, *Chem. Mater.* **2021**, *33*, 1444–1454.
[14] a) C. Jia, F. G. Cirujano, B. Bueken, B. Claes, D. Jonckheere, K. M. van Geem, D. de Vos, *ChemSusChem* **2019**, *12*, 1256–1266; b) X. Yan, K. Wang, X. Xu, S. Wang, Q. Ning, W. Xiao, N. Zhang, Z. Chen, C. Chen, *Inorg. Chem.* **2018**, *57*, 8033–8036.
[15] a) X. He, B. G. Looker, K. T. Dinh, A. W. Stubbs, T. Chen, R. J. Meyer, P. Serna, Y. Román-Leshkov, K. M. Lancaster, M. Dincă, *ACS Catal.* **2020**, *10*, 7820–7825; b) C. Castillo-Blas, I. Romero-Muñiz, A. Mavrandonakis, L. Simonelli, A. E. Platero-Prats, *Chem. Commun.* **2020**, *56*, 15615–15618; c) W. Jumpathong, T. Pila, Y. Lekjing, P. Chirawatkul, B. Boekfa, S. Horike, K. Kongpatpanich, *APL Mater.* **2019**, *7*, 111109.
[16] P. S. Bojan Kozlevcar, *Croat. Chem. Acta* **2008**, *81*, 369–379.
[17] A. R. Fahami, T. Günter, D. E. Doronkin, M. Casapu, D. Zengel, T. H. Vuong, M. Simon, F. Breher, A. V. Kucherov, A. Brückner, J.-D. Grunwaldt, *React. Chem. Eng.* **2019**, *4*, 1000–1018.
[18] K. J. Wallace, S. R. Cordero, C. P. Tan, V. M. Lynch, E. V. Anslyn, *Sens. Actuators B* **2007**, *120*, 362–367.
[19] B. Bolić, A. Mijušković, A. Popović-Bijelić, A. Nikolić-Kokić, S. Spasić, D. Blagojević, M. B. Spasić, I. Spasojević, *Nitric Oxide* **2015**, *51*, 19–23.
[20] M. Schulz, A. Gehl, J. Schlenkrich, H. A. Schulze, S. Zimmermann, A. Schaate, *Angew. Chem. Int. Ed.* **2018**, *57*, 12961–12965; *Angew. Chem.* **2018**, *130*, 13143–13147.

Manuscript received: February 24, 2023
Revised manuscript received: February 28, 2023
Accepted manuscript online: March 6, 2023